

Incremental Training of Graph Neural Networks on Temporal Graphs under Distribution Shift

Lukas Galke¹[0000–0001–6124–1092], Iacopo Vagliano³[0000–0002–3066–9464], and
Ansgar Scherp⁴[0000–0002–2653–9245]

¹ Kiel University, Germany lga@informatik.uni-kiel.de

² ZBW, Germany l.galke@zbw.eu

³ Amsterdam University Medical Center, Netherlands i.vagliano@amsterdamumc.nl

⁴ Ulm University, Germany ansgar.scherp@uni-ulm.de

Abstract. Current graph neural networks (GNNs) are promising, especially when the entire graph is known for training. However, it is not yet clear how to efficiently train GNNs on temporal graphs, where new vertices, edges, and even classes appear over time. We face two challenges: First, shifts in the label distribution (including the appearance of new labels), which require adapting the model. Second, the growth of the graph, which makes it, at some point, infeasible to train over all vertices and edges. We address these issues by applying a sliding window technique, i.e., we incrementally train GNNs on limited window sizes and analyze their performance. For our experiments, we have compiled three new temporal graph datasets based on scientific publications and evaluate isotropic and anisotropic GNN architectures. Our results show that both GNN types provide good results even for a window size of just 1 time step. With window sizes of 3 to 4 time steps, GNNs achieve at least 95% accuracy compared to using the entire timeline of the graph. With window sizes of 6 or 8, at least 99% accuracy could be retained. These discoveries have direct consequences for training GNNs over temporal graphs. We provide the code (<https://github.com/Incremental-GNNs>) and the newly compiled datasets (<https://zenodo.org/record/3764770>) for reproducibility and reuse.

Keywords: machine learning · graph neural networks · temporal graphs

1 Introduction

Graph neural networks (GNNs) achieve promising results on tasks such as node classification [14,28], link prediction [13], edge classification[19], collaborative filtering [1], and unsupervised representation learning [29]. So far, the datasets employed in those tasks are mostly static snapshots of graphs. However, an interesting property of GNNs is that they can deal with previously unseen vertices and edges, or even be applied to completely new graphs. This is a conceptual advantage over other approaches, which motivates to explore how graph neural networks can be applied to temporal graphs.

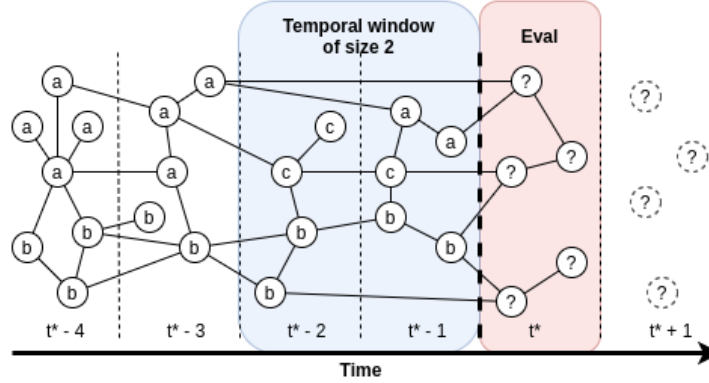


Fig. 1: A temporal graph where new vertices appear over time. New edges may occur within a single or across multiple time steps. New classes may appear over time, e.g., class c first appears at $t^* - 2$. Training is constrained on the visible window size. The vertices at timestep t^* are to be annotated with a class label from the set $\{a, b, c\}$, before advancing to the next time step.

We consider a temporal graph to be a series of snapshots $(\mathcal{G}_t)_{t \in \mathbb{N}}$. In each *time step* t , previously unseen vertices and edges and even new classes may appear (see Figure 1). For these temporal graphs, we investigate training graph neural networks for the node classification task, i.e., assigning class labels \mathbf{y} to previously unseen vertices based on vertex attributes \mathbf{X} and connections to other vertices via edges. A key challenge is that temporal graphs are growing larger and larger and memory becomes an issue over time. This is especially important for graph neural networks as the graph has to fit in memory to make predictions. Therefore, it may become necessary to cut off the history of past vertices (and their edges) depending on available resources. We denote the history of vertices and edges we take into account as the *temporal window*. The temporal window spans a range of multiple time steps, which we denote as the *temporal window size*. Another crucial challenge in our temporal setting is the *distribution shift*. Over time, the label distribution $p(\mathbf{y}|\mathcal{G}, \mathbf{X})$ may change and new classes may appear. This suggests that it is necessary to adapt models over time.

For example, consider the node classification task on a graph of scientific publications, where vertices represent papers and edges represent citations. Every year, the graph is expanded by new publications and citations. The goal is to classify the new publications into topics based on their title and their citations. Over time, also new topics, i.e. classes, may emerge and the model has to adapt. With a temporal window approach and an exemplifying window of 5 years, we would discard all publications and corresponding citations that are older than 5 years. We perform some training epochs on this window and subsequently make a prediction for the publications of the next year. Multiple research questions arise when training GNNs in such temporal scenarios:

- Q1** How long is a once-trained, static model sufficiently accurate?
Q2 Is it beneficial to reuse model parameters from the previous time step?
Q3 How far do we need to look into the past, such that we can match the accuracy of a model that uses the entire timeline of the graph?

To answer these questions, we compare static models vs incrementally trained models, compare reusing parameters (*warm restart*) vs random reinitialization (*cold restart*), and finally, compare incremental training with limited window sizes against using unlimited window sizes in each incremental step.

We apply this experimental procedure to three newly compiled temporal graph datasets based on scientific publications: two citation graphs based on DBLP and one co-authorship graph based on Web of Science. We select two representative GNN architectures: GraphSAGE-mean and graph attention networks along with graph-agnostic multi-layer perceptrons. With the goal of dataset-agnostic results, we select candidate window sizes based on characteristics of the respective dataset. We determined window sizes of 1, 3, and 6 time steps for the two DBLP datasets, and 1, 4, 8 for the Web of Science dataset.

The results of our experiments show that already a small window size of 3 or 4 time steps, GNNs achieve at least 95% accuracy compared to using an infinite temporal window size. With window sizes of 6 or 8, 99% accuracy can be retained. Our experiments further confirm that incremental training is necessary to account for distribution shift in temporal graphs. The question of reusing parameters from the previous time step depends on the dataset and the strength of the distribution shift: the more classes appear or disappear over time, the better becomes random reinitialization over reusing parameters from previous time steps. In summary, our contributions are:

- We introduce three novel temporal graph datasets for the node classification task: one based on the co-authorship graph and two based on citation data.
- We show that incremental training is necessary to account for distribution shift on temporal graphs and analyze the effect of reusing parameters from previous time steps.
- We relate window sizes to their coverage of the receptive field of graph neural networks. When 50% of the receptive field is inside the temporal window, GNNs achieve 95% accuracy compared to using the entire timeline of the graph. With 75% of the receptive field, 99% of the accuracy can be retained.

The remainder of this paper is organized as follows: We present the main related works in Section 2. We describe the experimental procedure (Section 3.1), the employed models (Section 3.2), the relation with the receptive field (Section 3.3) and the datasets (Section 3.4). In Section 4, we outline the experiments and provide the results, which are discussed in Section 5, before we conclude.

2 Related work

We first provide the related work on GNNs for static graphs. Subsequently, we outline GNNs and other approaches for dynamic graphs.

Regarding static graphs, Dwivedi et al. [5] have introduced a benchmarking framework to re-evaluate several recent GNN variants. Dwivedi et al. further distinguish between isotropic and anisotropic GNNs. In isotropic GNNs, all edges are treated equally. Apart from graph convolutional networks [14], examples of isotropic GNNs are GraphSAGE-mean (GS-Mean) [10], DiffPool [32], and GIN [30]. Graph convolutional networks aggregate neighbor representations via their mean and introduce an artificial self-loop if not present. GS-Mean concatenates the vertices’ own representation to the aggregated neighbor representations before applying the parameters. In DiffPool, the authors propose a differentiable pooling module that can generate hierarchical representations of graphs, which is important for whole-graph classification. In GIN, the authors analyze the expressive power of different pooling operators and also introduce a specific treatment for the vertices’ own representations via a learnable parameter. In anisotropic GNNs, the weights for edges are computed dynamically. Instances of anisotropic GNNs include graph attention networks (GAT) [28], GatedGCN [2] and MoNet [17]. GATs use an attention mechanism to compute edge weights based on source and target representations. In GatedGCN, the authors propose a combination of TreeLSTMs [24] and graph convolutional modules [22]. In MoNet, the authors regard the convolution operation as a Gaussian mixture model with learnable parameters. Dwivedi et al. conclude that treatment of the vertices’ self-information, attention, hierarchy, or gating, are important factors for GNNs, and that residual connections [31] are necessary for deeper GNNs.

Most of the discussed works require having the whole graph in memory. Only GraphSAGE [10] uses neighbor sampling, in which a rooted subtree is spanned in the vertices of the current batch. Other sampling techniques have been proposed by Chen et al. [3] and Huang et al. [11]. Huang et al. propose an adaptive sampling approach with skip-connections to preserve first-order proximity. Chen et al. use control variate based sampling approach for stochastic training by keeping track of activations from previous sampling epochs. Other works such as ClusterGCN [4] and GraphSAINT [33] suggest to sample entire sub-graphs before applying the GNNs. These sampling approaches may be used in combination with our approaches of training with limited window sizes.

Regarding *dynamic graphs*, several works consider a fixed vertex set and stack recurrent modules on top of graph convolutional modules [23,15]. DySAT [21] also assumes a fixed vertex set and jointly employs self-attention over structural and temporal dimensions. EvolveGCN [19] learns a recurrent network to predict the parameters of a GCN for the next time step, such that vertex addition and removal is possible. Apart from graph neural networks, other approaches for dynamic graphs have been proposed. DynGEM [9] uses deep autoencoders to jointly minimize reconstruction loss between t and $t+1$ and embedding distance between connected vertices. Dyngraph2vec [8] extends this idea and introduces additional variants with recurrent decoders. Know-Evolve [26] relies on vertex embeddings and multivariate point processes. DyRep [27] extend this approach to better capture temporal dynamics. Only DynGEM and dyngraph2vec can deal with new vertices, while others are limited to a fixed vertex set.

In summary, most related work on GNNs for dynamic graphs make the assumption of having a fixed vertex set. Only EvolveGCN is suited to cope with vertex addition and removal. However, in the present work we focus on the distribution shift scenario, where new classes appear over time. To adapt EvolveGCN to deal with new classes, one would have to increase the number of hidden units of the RNN as these are tied to the parameters of the GCN. This is particularly challenging because of the recurrent connections in the RNN. In case of standard GNNs, we can separate class-specific parameters in the output layer of the GNN, such that we can perform a warm restart, even when new classes appear. Therefore, we analyze the properties of incrementally training standard GNN on temporal graphs.

3 Methods and Datasets

We state our problem as temporal node classification and briefly describe the employed graph neural networks. Subsequently, we introduce a measure for the distribution of temporal differences that is used to determine the temporal window sizes for the datasets. Finally, we illustrate the newly compiled datasets.

3.1 Preliminaries and Experimental Procedure

Preliminary Definitions Let $\mathcal{G}_t = (V_t, E_t)$ be a temporal graph with vertices V_t and edges E_t at time steps $t \in \mathbb{N}$. Thus, V_t is the (finite) set of vertices that are in the graph at time step t , and E_t the corresponding edges at time step t . Furthermore, we define the set of all vertices $V ::= \bigcup_{t \in \mathbb{N}} V_t$ and all edges $E ::= \bigcup_{t \in \mathbb{N}} E_t$, i. e., $\mathcal{G} = (V, E)$. We assume that the graph is monotonously growing, i. e., it holds for all $t \in \mathbb{N}$ that $V_t \subseteq V_{t+1}$ and $E_t \subseteq E_{t+1}$. This assumption does not impact the generality of our approach. Let $\text{ts}_{\min} : V \rightarrow \mathbb{N}$ be a function that returns for each vertex $v \in V$ the timestamp at which the vertex was added to the graph, i. e., $\text{ts}_{\min} : v \mapsto \min\{t \in \mathbb{N} | v \in V_t\}$. Finally, for each vertex $v \in V$ we have a feature vector $\mathbf{X}_v \in \mathbb{R}^D$ and a class label $\mathbf{y}_v \in \mathbb{N} < C$, where D is the number of vertex features and $C ::= \bigcup_{t \in \mathbb{N}} C_t$ is the global set of classes.

Experimental Procedure We train the neural network model over the graph’s vertices and edges that fall within a specified, limited time window. Subsequently, the model predicts the classes of the newly added vertices and edges at time step t^* . When advancing from one time step to the next, i. e., when moving the time window, the latest additions become part of the data for incremental training in the following time steps. Furthermore, the oldest vertices and edges fall out of the time window and are not used for the incremental training anymore. As baseline, we train over the entire timeline of the graph (unlimited window size).

Formally, we define the evaluation procedure as follows: For each evaluation time step $t^* \in [t_{\text{start}}, t_{\text{end}}]$, (1) we construct a subgraph $\tilde{\mathcal{G}} = (\tilde{V}, \tilde{E})$ of \mathcal{G} induced on $\tilde{V} = \{v \in V | t^* - c \leq \text{ts}_{\min}(v) \leq t^*\}$ and $\tilde{E} = \{(u, v) \in E \mid u, v \in \tilde{V}\}$. (2) We supply the competing models with the subgraph $\tilde{\mathcal{G}}$, the corresponding

vertex features, and labels for vertices $\{u \in \tilde{V} \mid \text{ts}_{\min}(u) < t^*\}$ along with an epoch budget for updating their parameters. The task is to predict the labels for vertices $\{u \in \tilde{V} \mid \text{ts}_{\min}(u) = t^*\}$. (3) Finally, we measure the performance of the model in terms of accuracy. Subsequently, we move the temporal window by incrementing t^* and return to (1).

The temporal window size c is linked to the effective memory consumption as it controls the size of the respective subgraph. In practice, \mathcal{G} does not need to be known in advance: new vertices, edges, and classes can be dynamically inserted. Please note that the unlabeled data of the current evaluation time step is also visible during incremental training. We assume that we receive data in batches and make predictions after a full batch has arrived.

When advancing from one time step to the next, we consider two options of initializing the model. Using *cold restarts* corresponds to randomly re-initializing each model in each time step and training it from scratch [6]. In contrast, when using *warm restarts*, one takes the final weights of the previous time step as initialization for the next time step [6]. When new classes appear, we initialize the additional parameters in the output layer randomly, also in the warm restart case. Algorithm 1 implements our experimental procedure.

Data: Temporal graph \mathcal{G} , features \mathbf{X} , labels \mathbf{y} , time steps t , temporal window size c , epoch budget n_{epochs}

Result: Predicted class labels for vertices in each time step of the graph

```

known_classes  $\leftarrow \emptyset$ ;
 $\theta \leftarrow \text{initialize\_parameters}()$ ;
for  $t^* \leftarrow t_{\text{start}}$  to  $t_{\text{end}}$  do
     $\tilde{\mathcal{G}} \leftarrow$  subgraph of  $\mathcal{G}$  induced on vertices  $u$ , where  $t^* - c \leq \text{ts}_{\min}(u) \leq t^*$ ;
     $\tilde{\mathbf{y}}_{\text{train}} \leftarrow \tilde{\mathbf{y}}_u$ , where  $\text{ts}_{\min}(u) < t^*$ ;
    new_classes  $\leftarrow \text{set}(\tilde{\mathbf{y}}_{\text{train}}) \setminus \text{known\_classes}$ ;
    if do_cold_restart then
        // Cold restart
         $\theta \leftarrow \text{initialize\_parameters}()$ ;
    else
        // Warm restart
        tmp  $\leftarrow \text{clone}(\theta)$ ;
         $\theta \leftarrow \text{initialize\_parameters}()$ ;
         $\theta_{|\text{new\_classes}|} \leftarrow \text{tmp}_{|\text{new\_classes}|}$ ;
    end
     $\theta \leftarrow \text{train}(\theta, \tilde{\mathcal{G}}, \tilde{\mathbf{X}}, \tilde{\mathbf{y}}_{\text{train}})$  for  $n_{\text{epochs}}$  epochs;
     $\tilde{\mathbf{y}}_{\text{pred}} \leftarrow \text{predict}(\theta, \tilde{\mathcal{G}}, \tilde{\mathbf{X}})$  for vertices  $u$ , where  $\text{ts}_{\min}(u) = t^*$ ;
    known_classes  $\leftarrow \text{known\_classes} \cup \text{new\_classes}$ ;
end

```

Algorithm 1: Incremental training procedure of our experimental apparatus

3.2 Graph Neural Networks

We introduce and motivate our choice of representative architectures of graph neural networks employed in our experiments. We adopt the categorization between isotropic and anisotropic GNNs, as outlined in the Section 2 and select one representative for each type. We select GraphSAGE-Mean (GS-Mean) [10] as a representative for isotropic GNNs because its special treatment of the vertices’ own information has shown to be beneficial [5]. GS-mean concatenates the current vertices own representation to averaged neighbors’ representations before multiplying with the parameters \mathbf{U} . In GS-Mean, the procedure to obtain representations in layer $l + 1$ for vertex i is given by the equations:

$$\hat{\mathbf{h}}_i^{l+1} = \mathbf{h}_i^l \parallel \frac{1}{\deg_i} \sum_{j \in \mathcal{N}(i)} \mathbf{h}_j^l \quad \mathbf{h}_i^{l+1} = \sigma(\mathbf{U}^l \hat{\mathbf{h}}_i^{l+1})$$

where $\mathcal{N}(i)$ is the set of adjacent vertices to vertex i , \mathbf{U}^l are the parameters of layer l , σ is a non-linear activation function, and $\cdot \parallel \cdot$ is the concatenation. Bias parameters omitted for clarity.

For anisotropic GNNs, we select graph attention networks (GATs) [28] as our representative. All variants of anisotropic GNNs considered in Dwivedi et al. [5] are accurate and show only minor dataset-dependent differences. We chose GAT because it seems to be most commonly reused in the literature. In GATs, representations in layer $l + 1$ for vertex i are computed by the equations:

$$\hat{\mathbf{h}}_i^{l+1} = w_i^l \mathbf{h}_i^l + \sum_{j \in \mathcal{N}(i)} w_{ij}^l \mathbf{h}_j^l \quad \mathbf{h}_i^{l+1} = \sigma(\mathbf{U}^l \hat{\mathbf{h}}_i^{l+1})$$

where the edge weights w_{ij} and self-connection weights w_i are computed by a self-attention mechanism based on the representations \mathbf{h}_i and \mathbf{h}_j , i.e., the softmax of $a(\mathbf{U}^l \mathbf{h}_i \parallel \mathbf{U}^l \mathbf{h}_j)$ over edges, where a is a single layer neural network with LeakyReLU activation. We refer to the original work [28] for more details.

3.3 Measure for the Coverage of Receptive Fields

When k graph convolution layers are used, the features within the k -hop neighborhood of each vertex are taken into account for its representation in layer k . This k -hop neighborhood is referred to as the *receptive field* of a GNN [3]. When we incrementally train GNNs on a sliding window through time, the window size determines which vertices are available both for training and for inference. Ideally, the temporal window covers all vertices within the GNN’s receptive field, such that GNNs have access to all relevant information. Larger window sizes, however, come with increased memory requirements.

How many vertices of the receptive field are covered by windows of a specific size depends on the characteristics of the datasets. For this reason, we introduce a measure, $\mathbb{C}_{\Delta t}^k$, that gives a distribution of temporal distances within the receptive field of a GNN with k -graph convolution layers. Let $\mathcal{N}_k(u)$ be the k -hop

neighborhood of u , i. e., the set of vertices that are reachable from u by traversing at most k edges. Then, we define $\mathbb{C}_{\Delta t}^k(\mathcal{G})$ to be the multiset of time differences to past vertices:

$$\mathbb{C}_{\Delta t}^k(\mathcal{G}) := \{\text{ts}_{\min}(u) - \text{ts}_{\min}(v) | u \in V \wedge v \in \mathcal{N}^k(u) \wedge \text{ts}_{\min}(u) \geq \text{ts}_{\min}(v)\} \quad (1)$$

This distribution can be computed via breadth-first-search in $\mathcal{O}(b^{k+1})$ time, where b is the average out-degree. When the multiset is stored via counts, space complexity is $\mathcal{O}(|V| + T)$, where T is the maximum number of time steps. Please note that this is a dataset-specific measure to determine comparable window sizes. It needs to be computed only once, prior to any training iterations. When we consider a GNN with k graph convolution layers, the distribution $\mathbb{C}_{\Delta t}^k$ enumerates the temporal differences within the receptive field of the GNN. In our experiments, we will use the 25th, 50th, and 75th percentiles of this dataset-specific distribution for analyzing the effect of the temporal window size, which corresponds a receptive field coverage of 25%, 50%, and 75%, on average.

3.4 Datasets

We compile three new temporal graph datasets based on scientific publications: one co-authorship graph (PharmaBio) and two citation graphs (DBLP-easy and DBLP-hard). Table 1 shows the basic characteristics of the datasets.

PharmaBio To compile the PharmaBio dataset, we use the metadata of 543,853 papers by Pharma and Biotech companies from Web of Science [16]. After removing duplicates, our data cleaning procedure ensures that there is a certain amount of labels for each class per year and that each paper is connected to at least one other paper by a same-author edge. More specifically, we: (1) Keep only papers that are in a journal category with at least 20 papers per year; (2) Keep only papers where at least one of the authors has at least two papers per year; (3) Create vocabulary of words (regular expression: `\w\w+`) that appear in at least 20 papers globally and keep only papers with at least one of these words. We iterate steps 1–3 until no further paper has been removed in one pass. We end up with 68,068 papers from 23,689 authors working for 68 companies. These papers are distributed across 2,818 journals which are, in turn, categorized into seven journal categories. During preprocessing, each paper becomes a vertex in the graph. The class of the paper is the category of the journal in which it was published. We insert an edge between two vertices, if they share at least one common author (based on string comparison).

DBLP-easy and DBLP-hard To compile these datasets, we use the DBLP Citation Network dataset (version 10)⁵ [25] as a basis. It comprises 3M citing documents and 25M citations to 2M distinct cited documents, ranging between years. We use venues (conferences or journals) as class labels and use citations as edges. First, we select the subset from 1990 until 2015. Then, we follow a similar

⁵ <https://aminer.org/citation>

Table 1: Total number of vertices $|V|$, number of edges $|E|$ excluding self-loops, est. power law exponent α , number of features D and number of classes $|C|$, number of newly appearing classes within the evaluation time steps $|C_{\text{new}}|$, the 25,50,75-percentiles of the distribution of temporal differences $\mathbb{C}_{\Delta t}^2$, along with the total number of time steps T for our considered datasets.

Dataset	$ V $	$ E $	α	D	$ C $	$ C_{\text{new}} $	25% $\mathbb{C}_{\Delta t}^2$	50% $\mathbb{C}_{\Delta t}^2$	75% $\mathbb{C}_{\Delta t}^2$	T
PharmaBio	68,068	2,1M	1.4592	4,829	7	0	1	4	8	21
DBLP-easy	45,407	112,131	1.9300	2,278	12	3	1	3	6	25
DBLP-hard	198,675	643,734	1.7345	4,043	73	23	1	3	6	25

procedure as above: (1) Keep only papers from venues that have at least τ_{venue} papers in each year they occur (may be only every second year). (2) Keep only papers that stand in at least one citation relation to another paper. (3) Remove papers from venues that occur only in a single year. (4) Keep only papers with at least one word from a vocabulary of words that are in at least τ_{words} papers. We iterate steps 1–4 until no further paper has been removed in one pass. The difference between DBLP-easy and DBLP-hard is that $\tau_{\text{venue}} := 100$ papers in the easy variant and $\tau_{\text{venue}} := 45$ papers in the hard variant. The minimum word occurrence threshold τ_{words} is set to 20 for DBLP-easy and 40 for DBLP-hard. Finally, we construct the graph with papers as vertices, citations as edges, and venues as classes.

Table 1 shows the resulting dataset characteristics. For all three datasets, we use L2-normalized *tf-idf* [20] representations as vertex features based the corresponding papers’ title. We estimate the power law coefficient α via maximum likelihood [18] $\alpha = 1 + n \left(\sum_{u \in V} \ln \frac{\deg_u}{\deg_{\min}} \right)^{-1}$ where \deg_{\min} is 1 (2 for PharmaBio). In Figure 2, we visualize the degree distribution, label distribution, and the distribution over years. The distributions of temporal differences are visualized in Figure 3. All compiled datasets seem to follow a power law distribution, which is typical for citation and co-authorship graphs.

For each dataset, we chose the boundaries for our evaluation time steps $[t_{\text{start}}, t_{\text{end}}]$, such that 25% of the total number of vertices lie before t_{start} , and t_{end} is the final time step. For PharmaBio (1985–2016), that is $t_{\text{start}} = 1999$, and for both DBLP variants (1990–2015), that is $t_{\text{start}} = 2004$. Data before t_{start} may be used for training, depending on the window size. Regarding changes in the class set (distribution shift), DBLP-easy comprises 12 venues in total, including one bi-annual conference and four new venues appearing in the years 2005, 2006, 2007, and 2012. DBLP-hard comprises 73 venues, including one discontinued, nine bi-annual, six irregular venues, and 23 new venues, i. e. classes, within the evaluation time frame.

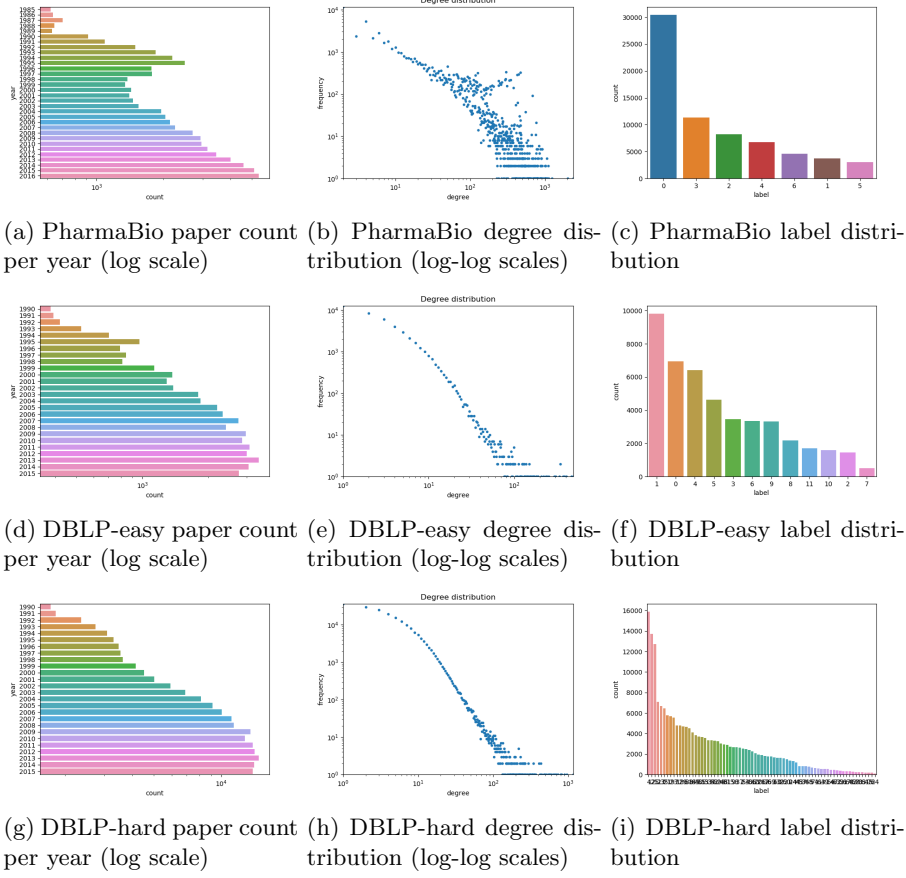


Fig. 2: Distribution of vertices per year, degree distributions, label distributions, for our temporal graph datasets.

3.5 Hyperparameter Choices and Evaluation Measures

We design the models to have a comparable capacity: one hidden layer with 64 hidden units. We use ReLU activation on the hidden layer of MLP and GS-Mean. GS-Mean has one hidden layer, i.e. two graph convolutional layers, with 32 units for self-connections and 32 units for aggregated neighbor representations. GAT has one hidden layer composed of 8 attention heads and 8 hidden units per head, along with one attention head for the output layer. We initialize the model parameters according to Glorot and Bengio [7]. We use dropout probability 0.5 on the hidden units for all models. We use Adam [12] to optimize for cross-entropy. We tune all learning rates on DBLP-easy with a search space of $\{10^{-1}, 5 \cdot 10^{-2}, 10^{-2}, 5 \cdot 10^{-3}, 10^{-3}, 5 \cdot 10^{-4}, 10^{-4}\}$. The learning rates are tuned separately for each model, each parameter reinitialization strategy, and

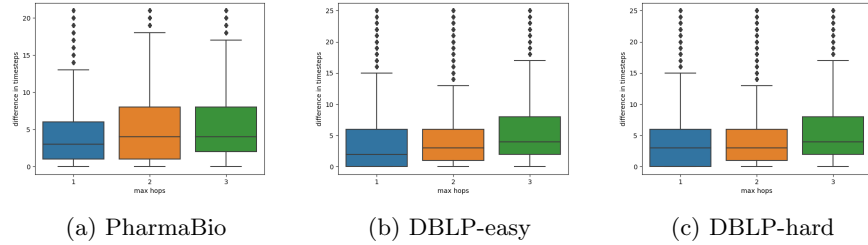


Fig. 3: Distributions of time differences $\mathbb{C}_{\Delta t}^k$ within the k -hop neighborhood of each vertex, corresponding to the receptive field of a k -layer GNN.

each window size. We do not use weight decay because it did not increase the performance (search space $\{0, 10^{-3}, 5 \cdot 10^{-4}, 10^{-4}, 5 \cdot 10^{-5}, 10^{-5}\}$). Our evaluation measure is accuracy, i.e., the fraction of correct predictions, in each time step. When aggregating results over time, we use the unweighted average. We repeat all experiments 10 times with different random seeds. We run each experiment on a single NVIDIA Titan X (Pascal) / Titan Xp GPU with 12GB memory. GS-Mean with unrestricted window size needed to run on CPU due to memory constraints. For implementation, we rely on PyTorch (pytorch.org) and the DGL (dgl.ai) framework.

4 Experiments and Results

In the following, we provide the results of our experiments on incremental training in the presence of distribution shift and limited temporal window sizes.

4.1 Distribution Shift and Incremental Training

In this experiment, we compare a once-trained static model against incrementally trained models. We train the static models for 400 epochs on the data before the first evaluation time step, which comprises 25% of the total vertices. We train incremental models for 200 epochs on temporal windows of 3 time steps (4 on the PharmaBio dataset) before evaluating each time step. The tuned initial learning rate is 10^{-3} for MLP and GS-Mean. For GATs, it is $5 \cdot 10^{-3}$ in the static case, and 10^{-2} with incremental training.

Figure 4 shows the results. We see that the accuracy of the static models decreases over time on DBLP-easy and DBLP-hard, where new classes appear over time. On PharmaBio, the accuracy of the static models stays on the same level, while the accuracy of incrementally trained models is increasing. Thereby, we empirically confirm shifts in the label distribution over time. In the next experiment, we only consider incrementally trained models.

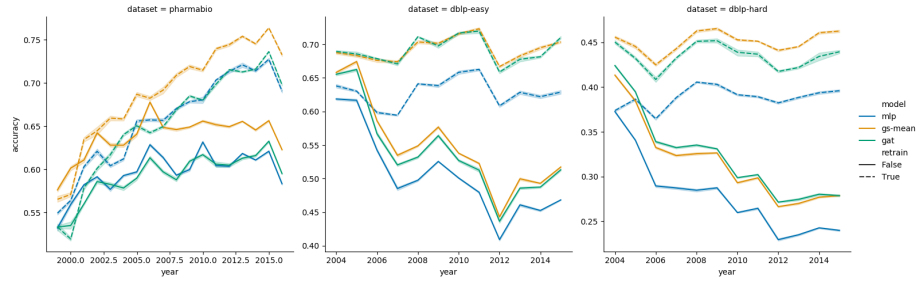


Fig. 4: **Incremental training to account for distribution shift.** Static models (solid lines) are trained for 400 epochs on 25% initial training data. Incrementally trained models are shown in dashed lines and are incrementally trained on windows of sizes 3 for DBLP-easy as well as DBLP-hard, and 4 for PharmaBio. Average accuracy of 10 different runs. Error regions are 95% confidence intervals computed with 1,000 bootstrap iterations over $N=2,520$ values.

4.2 Incremental Training and Effect of Different Window Sizes

First, we compare reusing the parameters of the model from the previous time step (warm restart) against randomly re-initializing the model parameters for each temporal window (cold restart). In both cases, we impose a 200 epoch budget per time step. The window size is set to 4 for PharmaBio and 3 for the two DBLP datasets, corresponding to 50% coverage of the GNNs’ receptive field. The tuned initial learning rate for MLP is 10^{-3} for both reinitialization strategies. For GS-Mean, we have 10^{-3} with warm start and $5 \cdot 10^{-3}$ with cold start. For GATs, we have 10^{-2} with warm start and $5 \cdot 10^{-3}$ with cold start.

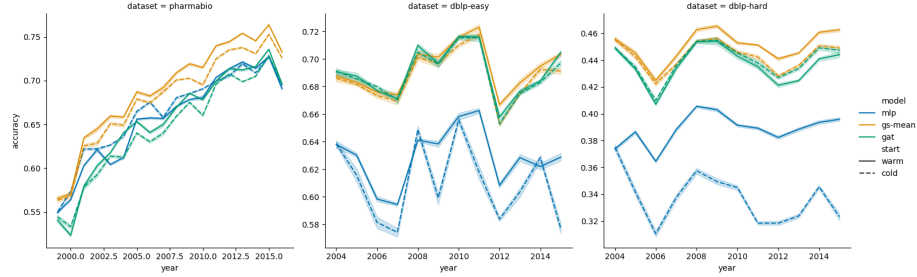


Fig. 5: **Cold vs warm restarts** in an online scenario with 200 epochs training over the window per time step. Average accuracy of 10 different runs. Error regions are 95% CI computed by 1,000 bootstrap iterations over $N=3,600$ values.

Figure 5 shows the results. On PharmaBio, warm restarts lead to more consistent accuracy scores than cold restarts for GNNs, while MLPs yield mixed

results. On DBLP-easy with 4 new classes, both cold and warm variants are close to each other with one exception: GS-Mean-warm suffers from a noticeable decrease during years 2006 and 2007, which is less apparent for GS-Mean-cold. On DBLP-hard, with 23 new classes, cold restarts yield higher scores than warm restarts for both GS-Mean and GAT. This effect is stronger for GS-Mean and inverted for MLPs.

In our final experiment for incremental training, we compare using different window sizes against using all available data, which is our baseline. We select three window sizes per dataset based on the distribution of temporal differences $\mathbb{C}_{\Delta t}^2$ (see Section 3.3). These correspond to the quartiles, such that the windows cover 25%, 50%, and 75% of the GNNs’ receptive field (RF) (see Table 1). Thus, we can compare window sizes across datasets with different characteristics, i. e., connectivity patterns through time and total number of time steps.

For the temporal window size of 50% RF, we reuse the same learning rates as above. For 25% RF, we use the following learning rates: 10^{-3} for MLP-cold, $5 \cdot 10^{-4}$ for MLP-warm, 10^{-3} for GS-Mean-cold, $5 \cdot 10^{-4}$ for GS-Mean-warm, $5 \cdot 10^{-3}$ for GAT-cold, 10^{-3} for GAT-warm. For 75% RF, we use 10^{-3} for both MLP variants as well as GS-Mean-warm, $5 \cdot 10^{-3}$ for GS-Mean-cold as well as GAT-cold, and 10^{-2} for GAT-warm. For unlimited window size (or 100% RF), we use 10^{-2} for both GS-Mean variants, $5 \cdot 10^{-2}$ for both GAT variants, $5 \cdot 10^{-3}$ for MLP-cold, and 10^{-3} for MLP-warm.

Figure 6 shows the results. We observe that those GNN variants trained on the full timeline of the graph (100% RF) yield the highest scores on DBLP-easy and DBLP-hard. There, GNNs with window size 1 (25% RF) yield lower scores than training with larger window sizes (50% and 75% RF). On PharmaBio, limited window sizes lead to higher scores than full-graph training in some time steps (especially with warm restarts). On all datasets, the scores for training with limited window sizes larger than 1 are close to the ones of full-graph training.

To quantify the effect of window size, we average the accuracy across all time steps (see Table 2). For each dataset, model, and window size, we list only the best reinitialization strategy. We observe that, for window sizes that cover 50% of the receptive field, GNNs (and also MLPs) achieve at least 95% classification accuracy compared to full-graph training. When 75% of the receptive field is covered by the temporal window, at least 99% accuracy could be retained in all datasets.

5 Discussion

Our main result is that incremental training with limited window sizes is as good as incremental training over the full timeline of the graph. With window sizes of 3 or 4 (50% receptive field coverage), GNNs achieve at least 95% accuracy compared to using all available data for incremental training. With window sizes 6 or 8 (75% receptive field coverage), at least 99% accuracy can be retained.

Furthermore, we investigate whether incremental training helps to tackle the challenges of distribution shifts by comparing against once-trained, static mod-

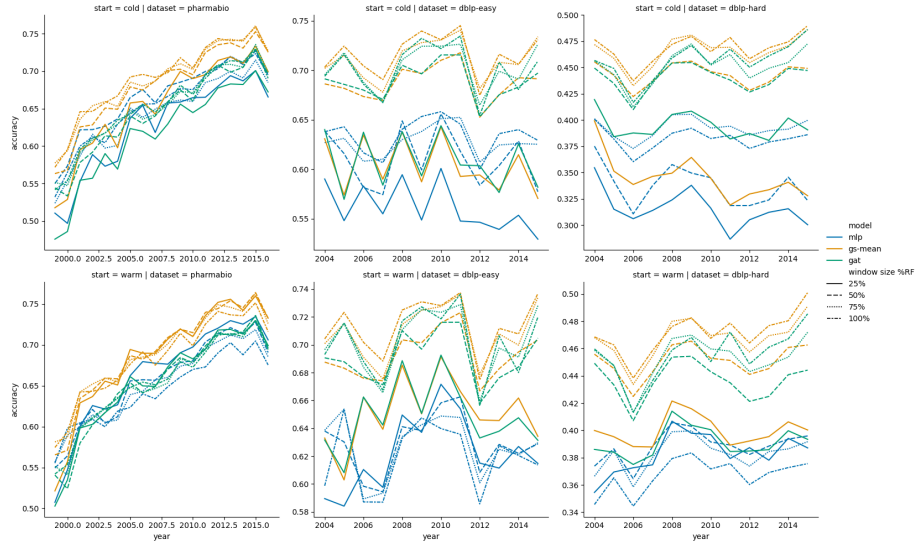


Fig. 6: **Comparison of different temporal window sizes** in an online scenario with 200 incremental training epochs per time step with either cold (*Top*) or warm restarts (*Bottom*) and varying temporal window sizes. 95% CI not shown for reasons of better visualization. Average accuracy of 10 different runs, resulting in 10,080 training and evaluation steps in total.

Table 2: Average accuracy across runs and time steps with varying temporal window sizes (c), 95% CI are computed based on sample variance (N=10,080). We list only the best performing values of cold (c) and warm (w) restarts for each configuration. We compare each average accuracy to the average accuracy obtained by training on the full graph (cmp. ∞).

dataset	c	gat		gs-mean		mlp	
		accuracy	cmp. ∞	accuracy	cmp. ∞	accuracy	cmp. ∞
dblp-easy	1 w:	.649 \pm .00	92%	w: .652 \pm .00	91%	w: .622 \pm .00	98%
	3 w:	.691 \pm .00	98%	w: .693 \pm .00	97%	w: .629 \pm .00	99%
	6 c:	.703 \pm .00	100%	c: .711 \pm .00	99%	c: .627 \pm .00	99%
	∞ w:	.702 \pm .00	100%	c: .716 \pm .00	100%	c: .634 \pm .00	100%
dblp-hard	1 c:	.394 \pm .00	86%	w: .400 \pm .00	85%	w: .383 \pm .00	100%
	3 c:	.440 \pm .00	96%	w: .451 \pm .00	96%	w: .389 \pm .00	102%
	6 w:	.453 \pm .00	99%	w: .467 \pm .00	99%	c: .392 \pm .00	103%
	∞ c:	.456 \pm .00	100%	w: .471 \pm .00	100%	c: .382 \pm .00	100%
pharmabio	1 w:	.654 \pm .01	100%	w: .686 \pm .01	99%	w: .663 \pm .01	101%
	4 w:	.653 \pm .01	100%	w: .690 \pm .01	100%	c: .663 \pm .01	101%
	8 w:	.654 \pm .01	100%	w: .690 \pm .01	100%	w: .653 \pm .01	100%
	∞ w:	.654 \pm .01	100%	c: .690 \pm .01	100%	c: .654 \pm .01	100%

els. On our dataset with a fixed class set, the performance of static models stays on the same level, while the performance of incrementally trained models increases. On datasets with new, unseen classes (DBLP-easy: 4, DBLP-hard: 23), the performance of static models decreases, while the performance of incrementally trained models stays on the same level. This confirms our expectations that static models suffer from distribution shift, while incrementally trained models can successfully adapt over time.

Our results for the reinitialization strategy are mixed. In a dedicated experiment with 50% receptive field coverage, we find that the stronger the distribution shift, i. e. the more changes within the class set, the better becomes the strategy of random reinitialization over reusing parameters. In future work, one could investigate deciding independently in each time step whether to perform a cold or a warm restart based on the amount of changes in that specific time step.

We have selected the candidate window sizes according to percentiles of the dataset-specific distribution of temporal differences. Absolute temporal window sizes may not generalize to other datasets. However, we expect that our results generalize when the window sizes are determined based on the coverage of the receptive field. Additionally, in this paper we have focused on the node classification task. GNNs can also be employed for link prediction [13], edge classification [19], or unsupervised representation learning [29]. Since this requires only modifying output layer and loss function, our findings might generalize also to other tasks. This, however, needs to be confirmed in further studies.

To assign specific vertices to temporal windows, we have used the time of their first occurrence in the graph (computed with the ts_{\min} function). Until now, we did not issue a specific treatment for vertices that are explicitly deleted from the graph at some time. After all, citation graphs and co-author graphs are monotonously growing. Considering removal, we would rely on the fact that vertices will eventually drop out of the temporal window and become inaccessible for training. One could explore other functions instead of ts_{\min} such as using only vertices that occur in all time steps spanned by the temporal window.

Furthermore, our experimental setup consists of evaluating on vertices of consecutive time steps. For preparing the next time step, the models are allowed to retrain on the true labels from previous time steps. If this data is available depends on the use case, i. e., whether the true labels are available in the next time step. This is the case for citation data and co-author graphs as we consider in this paper. An interesting direction of future work would be to use only small fractions of labeled data each year. Finally, results from papers on sampling-based graph convolution such as [11,3] can be directly applied to our approach, too, as the sampling can be restricted to the window size given. This would further improve memory efficiency.

Temporal graphs occur in many real-world scenarios such as citation graphs, transaction graphs, and social graphs. Practitioners face a trade-off between memory requirements, which are tied to the temporal window size, and expected accuracy of their models. Until now, it was not clear, how GNNs can be trained efficiently in such scenarios. With the results of this paper, practitioners can use

our guidelines for training GNNs on temporal graphs. For researchers, we supply our newly compiled datasets along with an implementation for the experimental procedure, such that dedicated methods for temporal graphs with new vertices and new classes may be developed.

6 Conclusion

We have analyzed incremental training of GNNs on temporal graphs under distribution shift. We could show that already small window sizes of 3 or 4 time steps lead to 95% accuracy compared to training on the entire timeline of the graph. These window sizes correspond to 50% coverage of the GNN’s receptive field. When 75% of the GNN’s receptive field is inside the temporal window, even 99% of the accuracy can be retained. To gain these insights, we have compiled three new, reusable temporal graph datasets based on scientific publications. We have conducted 16,200 training and evaluation steps with two representative GNN architectures: GraphSAGE-mean and graph attention networks. Temporal graphs are highly relevant in practice: not only scientific publications but also social networks and transaction networks are inherently instances of (growing) temporal graphs. Therefore, our findings are highly relevant for practitioners and opens up numerous new research directions.

We provide the source code (<https://github.com/lgalke/Incremental-GNNs>) as well as the newly compiled datasets (<https://zenodo.org/record/3764770>) for reuse.

References

1. van den Berg, R., Kipf, T.N., Welling, M.: Graph convolutional matrix completion. CoRR **abs/1706.02263** (2017)
2. Bresson, X., Laurent, T.: Residual gated graph convnets. CoRR **abs/1711.07553** (2017)
3. Chen, J., Zhu, J., Song, L.: Stochastic training of graph convolutional networks with variance reduction. In: ICML (2018)
4. Chiang, W., Liu, X., Si, S., Li, Y., Bengio, S., Hsieh, C.: Cluster-gcn: An efficient algorithm for training deep and large graph convolutional networks. In: KDD. pp. 257–266. ACM (2019)
5. Dwivedi, V.P., Joshi, C.K., Laurent, T., Bengio, Y., Bresson, X.: Benchmarking graph neural networks. CoRR **abs/2003.00982** (2020)
6. Galke, L., Vagliano, I., Scherp, A.: Can graph neural networks go “online”? an analysis of pretraining and inference. In: ICLR Workshop (2019)
7. Glorot, X., Bengio, Y.: Understanding the difficulty of training deep feedforward neural networks. In: AISTATS 2010. JMLR Proceedings, vol. 9. JMLR.org (2010)
8. Goyal, P., Chhetri, S.R., Canedo, A.: dyngraph2vec: Capturing network dynamics using dynamic graph representation learning. Knowl.-Based Syst. **187** (2020)
9. Goyal, P., Kamra, N., He, X., Liu, Y.: Dyngem: Deep embedding method for dynamic graphs. CoRR **abs/1805.11273** (2018)
10. Hamilton, W.L., Ying, Z., Leskovec, J.: Inductive representation learning on large graphs. In: NeurIPS (2017)

11. Huang, W., Zhang, T., Rong, Y., Huang, J.: Adaptive sampling towards fast graph representation learning. In: NeurIPS (2018)
12. Kingma, D.P., Ba, J.: Adam: A method for stochastic optimization. CoRR **abs/1412.6980** (2014)
13. Kipf, T.N., Welling, M.: Variational graph auto-encoders. CoRR **abs/1611.07308** (2016)
14. Kipf, T.N., Welling, M.: Semi-supervised classification with graph convolutional networks. In: ICLR (2017)
15. Manessi, F., Rozza, A., Manzo, M.: Dynamic graph convolutional networks. Pattern Recognition **97** (2020)
16. Melnychuk, T., Wirsich, A., Schultz, C.: Effects of university-industry collaborations in basic research on different stages of pharmaceutical new product development. In: Innovation and Product Development Management Conference (2019)
17. Monti, F., Boscaini, D., Masci, J., Rodolà, E., Svoboda, J., Bronstein, M.M.: Geometric deep learning on graphs and manifolds using mixture model cnns. In: CVPR. IEEE Computer Society (2017)
18. Newman, M.E.: Power laws, pareto distributions and zipf’s law. Contemporary physics **46**(5) (2005)
19. Pareja, A., Domeniconi, G., Chen, J., Ma, T., Suzumura, T., Kanezashi, H., Kaler, T., Leisersen, C.E.: Evolvegc: Evolving graph convolutional networks for dynamic graphs. CoRR **abs/1902.10191** (2019)
20. Salton, G., Buckley, C.: Term-weighting approaches in automatic text retrieval. Information processing & management **24**(5) (1988)
21. Sankar, A., Wu, Y., Gou, L., Zhang, W., Yang, H.: Dysat: Deep neural representation learning on dynamic graphs via self-attention networks. In: WSDM (2020)
22. Scarselli, F., Gori, M., Tsoi, A.C., Hagenbuchner, M., Monfardini, G.: The graph neural network model. IEEE Trans. Neural Networks **20**(1) (2009)
23. Seo, Y., Defferrard, M., Vandergheynst, P., Bresson, X.: Structured sequence modeling with graph convolutional recurrent networks. In: ICONIP. Springer (2018)
24. Tai, K.S., Socher, R., Manning, C.D.: Improved semantic representations from tree-structured long short-term memory networks. In: ACL (2015)
25. Tang, J., Zhang, J., Yao, L., Li, J., Zhang, L., Su, Z.: Arnetminer: Extraction and mining of academic social networks. In: KDD ’08. ACM (2008)
26. Trivedi, R., Dai, H., Wang, Y., Song, L.: Know-evolve: Deep temporal reasoning for dynamic knowledge graphs. In: ICML (2017)
27. Trivedi, R., Farajtabar, M., Biswal, P., Zha, H.: Dyrep: Learning representations over dynamic graphs. In: ICLR (2019)
28. Veličković, P., Cucurull, G., Casanova, A., Romero, A., Liò, P., Bengio, Y.: Graph attention networks. In: ICLR (2018)
29. Veličković, P., Fedus, W., Hamilton, W.L., Li, P., Bengio, Y., Hjelm, R.D.: Deep graph infomax. In: ICLR (2019)
30. Xu, K., Hu, W., Leskovec, J., Jegelka, S.: How powerful are graph neural networks? In: ICLR (2019)
31. Xu, K., Li, C., Tian, Y., Sonobe, T., Kawarabayashi, K., Jegelka, S.: Representation learning on graphs with jumping knowledge networks. In: ICML (2018)
32. Ying, Z., You, J., Morris, C., Ren, X., Hamilton, W.L., Leskovec, J.: Hierarchical graph representation learning with differentiable pooling. In: NeurIPS (2018)
33. Zeng, H., Zhou, H., Srivastava, A., Kannan, R., Prasanna, V.K.: Graphsaint: Graph sampling based inductive learning method. In: ICLR. OpenReview.net (2020)